Journal of Colloid and Interface Science 363 (2011) 540–550

Contents lists available at SciVerse ScienceDirect

Journal of Colloid and Interface Science

www.elsevier.com/locate/jcis

Effect of nanoparticle aggregation at low concentrations of TiO_2 on the hydrophilicity, morphology, and fouling resistance of PES–TiO_2 membranes

Arcadio Sotto [a,b,*], Arman Boromand [b,c], Ruixin Zhang [b], Patricia Luis [b], Jesús M. Arsuaga [a], Jeonghwan Kim [d], Bart Van der Bruggen [b]

[a] Department of Chemical and Energy Technology, Rey Juan Carlos University, Madrid, Spain
[b] Department of Chemical Engineering, K.U. Leuven, Leuven, Belgium
[c] Center for Experimental Mechanics, University of Ljubljana, Ljubljana, Slovenia
[d] Department of Environmental Engineering, INHA University, Incheon, South Korea

ARTICLE INFO

Article history:
Received 2 June 2011
Accepted 29 July 2011
Available online 11 August 2011

Keywords:
Nanoparticle aggregation
Membrane fouling
Double layer interaction
PES–TiO_2

ABSTRACT

This paper reports the fabrication and characterization of polyethersulfone–TiO_2 (PES–TiO_2) nanoparticle composite membranes made from synthesis casting solution consisting of various compositions of polymer solvents (DMF and EtOH) and TiO_2 additive. The results also revealed that the membrane permeation and rejection rates, pore size, and porosity were dependent on the TiO_2 and EtOH concentrations. Nanoparticles were characterized by zeta potential measurements, TEM observations, and measurement of particle size distributions. Zeta potential measurements in aqueous solution demonstrated that the TiO_2 particles size is dominated by electric double layer interactions. Addition of EtOH promotes the increase of the clusters size as consequence of a double effect: reduction of the dielectric constant of solution and the depletion of the suspension field determined by the action of the polymer chains. The observed effects as result of EtOH addition and increase of TiO_2 concentration were similar: both procedures provoked an increase of macrovoid dimensions. The modified membranes by TiO_2 incorporation showed a structural change from a sponge-like to a finger-like structure. Strong correlations were observed between the hydrophilicity and the permeability of manufactured membranes. The formation mechanism of TiO_2-blended membranes was altered, in a similar way, as result of EtOH at different contents of nanoparticles. Fouling resistance of modified membranes was significantly improved showing that EtOH addition is a suitable procedure for the membrane performance improvement. The rejection potential of membranes is hardly affected by the nanoparticles and EtOH incorporation into the polymeric solution.

1. Introduction

Recently, the effect of incorporation of nanoparticles into the membrane structure on the fouling behavior of polymeric membranes has been widely studied [1]. Many nanoparticles, such as TiO_2, Al_2O_3, SiO_2, and ZrO_2 [2–5], have been used as inorganic additive into polymeric membranes, typically aiming at an antifouling effect. In order to increase the fouling resistance expected for such membranes, researchers have taken interest in membrane surface modification in view of improving some membrane surface properties such as hydrophilicity, roughness, permeability, and pore size [6–10]. In addition to chemical modifications, the membrane performance has been also improved by the addition of nanoparticles into polymeric membranes [11–13]. The composite (organic–inorganic) membrane can combine exceptional properties of organic and inorganic materials and offer specific advantages for the preparation of hybrid membranes with excellent separation performances, good thermal and chemical resistance, and especially, improving poor fouling resistance of polymeric membranes for the treatment of wastewater environments [14–16].

Titanium dioxide (TiO_2) has attracted considerable attention in this regard because of its stability, commercial availability, and ease of preparation. In addition, TiO_2 is considered to be an ideal choice as catalyst for water treatment due to the high oxidation power, photo-induced hydrophilicity, long-term photostability, high transparency in the visible range, good thermal and chemical stability, and non-toxicity [17]. Due to the super-hydrophilic properties of TiO_2, the incorporation of this type of nanoparticles into the membrane structure enhances the composite material affinity to the water and hence the membrane water permeation [1].

* Corresponding author. Fax: +32 91 488 7068.
E-mail address: arcadio.sotto@urjc.es (A. Sotto).

0021-9797/$ - see front matter © 2011 Elsevier Inc. All rights reserved.
doi:10.1016/j.jcis.2011.07.089

Among polymeric materials used for manufacturing ultrafiltration and nanofiltration membranes for wastewater treatment, polyethersulfone (PES) is attractive because of its good physical and chemical properties [13].

Previous studies have shown that membrane fouling of polymeric membranes was significantly mitigated by the introduction of TiO_2 nanoparticles into the polymeric material [18–20]. However, most of these studies proposed the addition of nanoparticles to the casting solution in a relatively high concentration, i.e., range above 1 wt.% [6]. Negative effects of high concentrations on the performance of the resulting membrane, however, have also been observed [1]. In the work of Wu et al. [11], the authors used a concentration of 0.3 wt.%, which is at the lower end. The membrane performance at TiO_2 contents below 0.3 wt.% is still not understood, which is a lack in the knowledge of this research field. Therefore, the effect of nanoparticle agglomeration on the performance of PES–TiO_2 membranes in the low concentration interval of nanoparticles is studied here.

In our previous work [21], the effect of the addition of a low TiO_2 concentration on the permeability and membrane fouling of PES membranes, manufactured using 1-methyl-2-pyrrolidone (NMP) as solvent for the polymer, was studied by casting different concentrations of the polymer. The results showed that the TiO_2-entrapped membranes have a more open structure and higher hydrophilicity and permeability as result of confirmed presence of nanoparticles. The unusually low range of TiO_2 concentrations proposed provided a significant improvement in the permeability and fouling resistance of blended membranes. However, undesirable effects such as aggregation were observed leading to less improved membrane performance, in some cases similar to the former control membranes. The agglomeration behavior and surface charge variation of nanoparticle dispersions can have a negative effect on the reactivity of nanomaterials [22]. Therefore, accurate characterization of nanoparticle dispersions becomes very important for its environmental applications.

In this work, the effect of the TiO_2 dispersion by using ethanol as co-solvent for the polymer, in addition to dimethylformamide (DMF) as the solvent, is explored. The effect of nanoparticle size and distribution is also unknown in this research field and studied only recently by Razmjou et al. [23] and Maximous et al. [24].

Based on the publications of Rahimpour et al. [6] and Li et al. [13], which both reported that Degussa P25 with 80% anatase phase could change the structure of the membrane significantly, without considering the nanoparticle dispersion effect, Razmjou et al. applied a chemical and mechanical modification of commercial Degussa P25 TiO_2 nanoparticles to avoid agglomeration of nanoparticles for concentrations above 2 wt.% in the casting solution. These authors found an optimum value for the water flux and fouling resistance for selected modification conditions. Maximous et al. observed a change in the structure of membranes depending on the metal oxide distribution [24].

Because other studies did not address the impact of the metal oxide distribution on the membrane performance, the present study tries to fill this gap by exploring the factors that alter the TiO_2 particle size distribution and therefore the properties and performance of composite PES–TiO_2 membranes manufactured at lower concentrations of TiO_2.

On the other hand, it is known that the interdiffusion velocity increases with addition of TiO2, leading to membranes with higher pore size and porosity [25,26]. This fact can be explained by a double effect: higher affinity of TiO_2 to water than to the polymer, so that the penetration velocity of water into a nascent composite membrane increases; and the hindrance of particles that affect negatively the interaction between polymer and solvent molecules and hence solvent molecules can diffuse more easily from the polymer matrix [26]. Therefore, this study aims at investigating the importance of both effects in order to discriminate which one of them is predominant on the permeation properties of membranes at lower contents of TiO_2 particles. To accomplish this objective was analyzed the effect of particle aggregation by two different procedures: increasing the number of particle dissolved into the polymeric solution, adding higher contents of TiO_2, and using an additional polymer co-solvent for the membrane synthesis, in this case ethanol, in order to alter the interaction between particles for a fixed concentration of them. To see the effect of solvent choice on particle size, we employed two different solvents for this study, DMF, and a mixture of DMF and EtOH.

In addition to characterization of synthesized TiO_2 nanoparticles, the membrane's hydrophilicity, permeability, porosity, thermal resistance, molecular weight cut-off, and fouling potential by using different concentrations of TiO_2 and ethanol as co-solvent for the polymer were determined.

2. Experimental

2.1. Materials

Polyethersulfone (PES, type Radel) supplied by Solvay (Belgium) was employed as the polymer matrix. N,N-dimethylformamide (DMF, 99.5%) and ethanol (EtOH, ACS) purchased from Sigma Aldrich (St. Louis, MO) and Merk (Germany), respectively, were used as polymer solvents (Table 1). The support layer (Viledon FO2471) used for the PES membrane manufacturing was obtained from Freudenberg (Weinheim, Germany).

Sigma–Aldrich humic acid (St. Louis, MO) was selected as a model organic foulant in this study. Humic substances are macromolecules that naturally occur in all environments in which vegetation is present. Humic acids (HA) represent 90% of dissolved organic carbon constituting a major component of natural organic matter that can be found in wastewater streams and refers to the fraction of humic substances obtained by chemical and biological degradation products from plant and animal residues [27,28].

Polyethylene glycols (PEGs) with increasing molar mass (400, 600, 800, 1500, 4000, 6000, and 8000) purchased from Scharlab, S.L were chosen to estimate the molecular weight cut-off (MWCO) of manufactured membranes. Their feed solutions were made by dissolving the appropriate chemical in pure particle-free Milli-Q water to achieve initial concentrations of 200 mg L^{-1}.

2.2. TiO_2 preparation and characterization

Titanium tetraisopropoxide (TTIP) was used as a precursor of TiO_2 nanoparticles. 0.125 mol of TTIP was added dropwise to 100 mL of deionized water under vigorous stirring at room temperature. The sol samples obtained by hydrolysis process were irradiated in an ultrasonic cleaning bath for 1 h. To hydrolyze the TTIP samples and obtain monodisperse TiO_2 particles, the samples were subsequently aged in a closed beaker at room temperature for 24 h. After aging, these samples were dried at 100 °C for 8 h in air to vaporize water. Dried gel samples obtained were calcinated further at 500 °C for 1 h. Surface analysis and microscopic analysis using XRD (X-ray Diffractometer system, DMAX-2500, Rigaku) and TEM

Table 1
Physico-chemical properties of solvents used in this study.

Solvent	Chemical formula	Dielectric constant	Density (g mL^{-1})	Dipole moment (D)
Water	H—O—H	80	1.000	1.85
Ethanol	CH_3—CH_2—OH	25.7	0.789	1.69
DMF	H—C(=O)N(CH_3)$_2$	41.3	0.944	3.82

(CM 200, Philips Inc.) showed that the synthesized TiO_2 particles were characterized as anatase with 25 nm particle diameter.

To determine the particle size distribution, a MasterSizer Laser Diffraction Particle Size Analyzer (Malvern Instrument Ltd., Malvern, England) was used. The size distribution was quantified as the relative volume of particles in size bands presented as size distribution curves (Malvern MasterSizer Micro Software v 2.19).

To examine the effect of solution pH on the hydrodynamic size, surface charge, and isolelectric point, TiO_2 was dispersed in Milli-Q water at 0.2 wt.% concentration and the solution pH was adjusted by adding HCl and NaOH. Titania nanoparticle dispersions were sonicated for 15 min using a bath sonicator (40 W, 50 Hz, Fisher Scientific Fairlawn, New Jersey) before the size and zeta potential measurement. All measurements were carried out at 25 °C, which was maintained by the instrument. Repeatability of all hydrodynamic size and zeta potential was verified with more than four measurements.

To determine the hydrodynamic size for polymeric solutions, were tested four organic solutions prepared as it is explained in Section 2.2 for two different contents of TiO_2 (0.1 and 0.2 wt.%) without and with EtOH. After stirring and sonication, the polymeric suspensions were cooled down in a water bath under stirring continuously until temperature of 25 °C has been reached. Repeatability of all hydrodynamic size and zeta potential was verified with more than four measurements.

2.3. Membrane preparation

PES was used as a membrane material, and TiO_2-entrapped membranes from 0.1 to 0.4 wt.% relative to casting solution were prepared by phase inversion [27]. The effect of ethanol (EtOH) used as co-solvent was explored for concentrations ranging from 1 to 4 wt.%. First, DMF and EtOH were mixed, and then TiO_2 powders were added and stirred at a low speed for 3 h with ultrasonic vibration to avoid the serious aggregation of particles. Finally, the casting solutions were prepared by dissolving PES powders in the above solutions. After stirred for 72 h, the casting solution was degassed at 25 °C for at least 24 h to remove air bubbles. A thin film of the polymer solution with a thickness of 250 μm was cast on a support with a filmograph (K4340 Automatic Film Applicator, Elcometer) at a speed mm s^{-1} in an atmosphere with controlled relative air humidity. The casted polymer was immersed in anonsolvent bath of distilled water at 25 °C, in which phase separation starts and the membrane is formed. The detailed preparation method is presented in our previous work [21].

2.4. Membrane characterization

A contact angle measuring system DSA 10 Mk2 (Krüss, Germany) was used to measure the water contact angle of the synthesized membranes. A water droplet was placed on a dry flat homogeneous membrane surface, and the contact angle between the water and membrane was measured until no further change was observed. The average contact angle for distilled water was determined in a series of eight measurements for each of the different membrane surfaces.

To visualize membrane surface characteristics, scanning electron microscopy (SEM) measurements were performed. SEM images were made with a Philips XL30 FEG instrument with an accelerating voltage of 20 keV. Cross-sections were prepared by fracturing the membranes in liquid nitrogen.

Porosity (P_r, %) was calculated by uptake water experiments as a function of the membrane weight using the following equation:

$$P_r(\%) = \left(\frac{W_w - W_d}{Sd\rho}\right) \times 100 \quad (1)$$

where W_w and W_d are the weights of a membrane at equilibrium, swelling and dry state, respectively; S the membrane area; d the thickness and ρ is the density of water. The membranes were immersed in water during 24 h prior to measurement of swelling state. The porosity data were the average values obtained for four samples of each membrane.

Thermogravimetric analysis scans were performed on a simultaneous TGA-DSC thermobalance (TGA-DCS1, Mettler-Toledo, S.A.E.). A flow of 100 mL min^{-1} of Nitrogen was employed as inert gas. The heating rate was 10 °C min^{-1} and the samples placed in a ceramic pan (70 μL of capacity). Thermal investigations were carried out to explore the thermal stability of manufactured membranes in correlation with the TiO_2 added amount. Measurements were carried out for three pieces of a flat sheet membrane for every type of membrane with standard deviation below ±0.2% of weight loss.

2.5. Permeation experiments

The manufactured membranes were characterized for water flux, pure water permeability, and solute rejection studies using a cross-flow filtration set-up [29]. Experiments were carried out on a laboratory scale filtration apparatus (Amafilter, Test Rig PSS1TZ) equipped with two TZA 944 membrane modules in parallel. The feed solution is pumped to both membrane modules by a three-stage membrane pump. The volume was 10 L, including 1.5 L in the tubes of installation. Circular flat sheet membranes with a diameter of 9 cm and an effective filtration area of 0.0059 m^2 were used in both membrane modules. A constant feed composition was achieved by recycling the retentate and permeate stream to the feed tank. During sampling, permeate was collected in a gradual cylinder and the permeate flux (J) was calculated from the time needed to obtain certain permeate volume.

In a typical run, membranes were compacted using Milli-Q water for 1–2 h at 20 bar until there was no further variation in permeate flux, then the water flux was recorded. In this way, the influence of compaction during filtration experiments could be avoided.

After compaction, the pure water permeability was determined by measuring the pure water flux (J_w) at different transmembrane pressures (ΔP) from 4 to 16 bar; the permeability was determined as the slope of the linear regression of the water flux as a function of transmembrane pressure. Rejections were measured at a transmembrane pressure of 10 bar. During the rejection experiments, samples of permeate and concentrate solutions were collected every 30 min during 3 h, after the membrane system reached constant permeate flow values.

Pure water permeabilities and PEG rejection were determined for a wide range of membranes. Four membrane coupons of the same membrane sheet for four membranes of each type were tested. Therefore, the obtained results are the average of 16 experimental values. The maximum experimental errors were below 5% and 8% for control and modified membranes, respectively.

2.6. Fouling experiments

Pre-filtration studies with Milli-Q water at 25 °C and 10 bar transmembrane pressure were conducted until a steaty-state flux (J_w^i) was observed. Subsequently, cross-flow filtration experiments were carried out for acid humic acids solution at a fixed concentration of 5 mg L^{-1} during 8 h at the same operational conditional used previously. After the HA filtration test, the membrane was washed with distilled water for 2 h. The permeation flux of Milli-Q water was measured after this cleaning procedure when the system reached the steaty-state flux (J_w^f).

To describe flux decline, the resistance-in-series model [23] was used. In this model, the water flux is written as a function of transmembrane pressure (ΔP), the viscosity (η), and the total membrane resistance (R_t):

$$J = \frac{\Delta P}{\eta R_t} \tag{2}$$

When filtering pure water, the resistance against mass transport only involves the membrane intrinsic resistance (R_m), whereas during filtration of a feed solution, the flux declines according to gel resistance layer formation (R_g) and the solute adsorption of macromolecules (foulants) on membrane pore wall or surface (R_f). This model has been successfully applied by other authors to study the membrane fouling performance [5,23].

Membrane resistances values can be obtained from experimental data using the following equations:

$$R_m = \frac{\Delta P}{\eta J_w^i} \tag{3}$$

$$R_f = \frac{\Delta P}{\eta J_w^f} - R_m \tag{4}$$

$$R_g = \frac{\Delta P}{\eta J_v} - (R_m + R_f) \tag{5}$$

$$R_t = R_m + R_f + R_g \tag{6}$$

The flux of the feed solution is defined as J_v, and the pure water flux measured before and after the filtration experiments is represented as J_w^i and J_w^f, respectively.

Flux decline can also be caused by cake formation that usually occurs during filtration of colloidal dispersion, due to accumulation of particles on the membrane surface. Another source of fouling can be the specific interactions between the membrane and the solute that can damage the membrane or change its properties. The effect of the two last ones resistances will not be considered in this investigation due to the characteristics of the synthetic solutions and the mild operational conditions used.

2.7. Analytical methods

The concentration of PEG's and saccharides solutions was measured with a Total Organic Carbon (TOC) analyzer (model TOC-V CSN Shimadzu). The rejection factor was determined as follows:

$$R(\%) = \left(1 - \frac{C_p}{C_f}\right) \times 100 \tag{7}$$

where C_p and C_f are the permeate and feed concentrations of PEGs, respectively.

To determine the concentration of TiO_2 nanoparticles in membrane structure, Inductively Coupled Plasma Atomic Emission Spectroscopy (ICP-AES, Agilent Technologies, CA, USA) was used. The PES membranes at different TiO_2 concentrations tested were characterized at 337 nm wavelength, corresponding to titania adsorption.

3. Results and discussion

3.1. Nanoparticles characterization

Transmission electron microscopy (TEM) was used to investigate the particle size as shown in Fig. 1. The TiO_2 particles can be seen in the form of black spots and the size ranges from 25 to 50 nm. It can be seen that some particles form larger clusters on the surface, which can be ascribed to the agglomeration of TiO_2 particles.

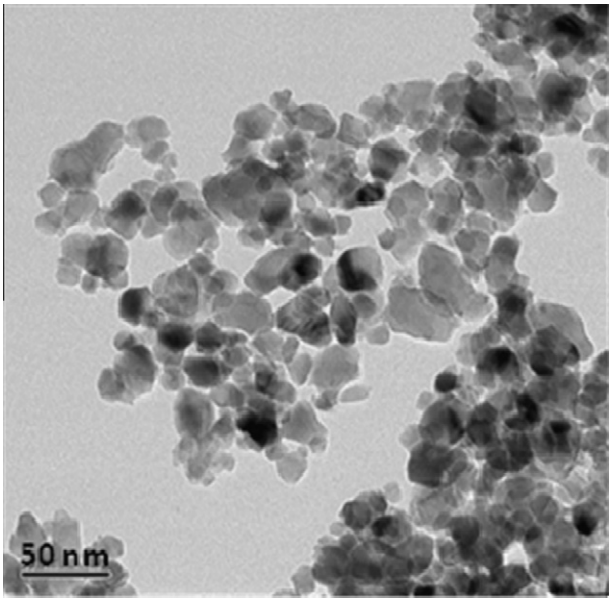

Fig. 1. TEM image of TiO_2 nanoparticles prepared by the sol–gel method.

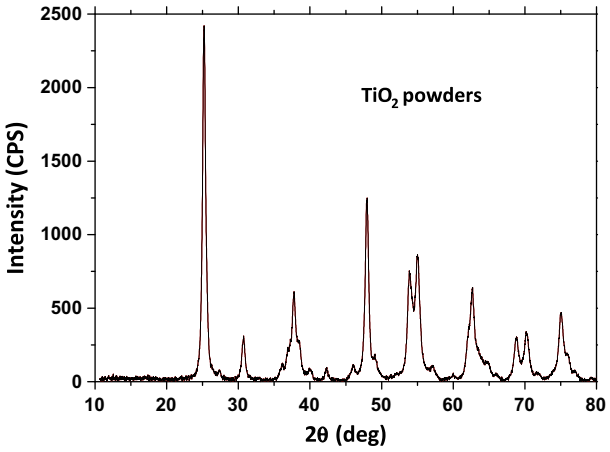

Fig. 2. XRD pattern of synthesized TiO_2 powders by sol–gel method.

The XRD analysis, used to characterize the crystal structure of TiO_2 particles, is shown in Fig. 2. Amorphous TiO_2 was used as starting material, and then the anatase appeared after calcinating at 550 °C. It is generally known that spherical TiO_2 nanoparticles with high surface area can be prepared by the sol–gel technique [30]. The anatase TiO_2 nanoparticle is known to be very photoactive and practical for oxidative water purification [31]. The structure of the polymeric PES membrane may be affected by TiO_2's inherent catalytic properties when oxidants are used in water while further studies are needed. However, this paper focuses on intrinsic effects of TiO_2 on membrane performance without any oxidant; the catalytic effect of TiO_2 on the PES membrane was not considered in this paper.

The zeta potential of the synthesized TiO_2 nanoparticles was measured for a aqueous solution containing 0.2 wt.% of TiO_2 at different pHs. Fig. 3 shows a typical amphoteric behavior of the electrophoretic mobility of TiO_2 nanoparticles as a function of solution pH. The pH dependence of the TiO_2 nanoparticles indicates an isoelectric point (IEP) around 6.2. At pH values above the IEP, the neg-

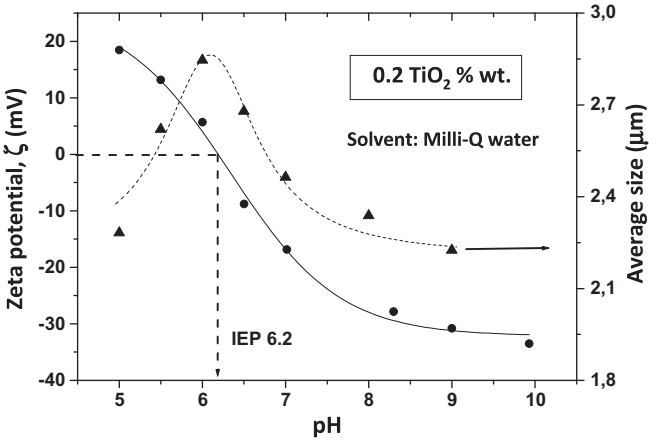

Fig. 3. Zeta potential (circles) and average size (triangles) of TiO_2 agglomerates as function of aqueous solution pH.

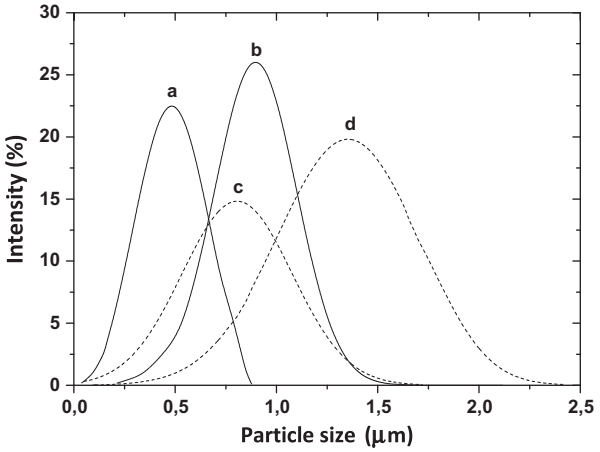

Fig. 4. TiO_2 particle size distribution in organic polymeric solutions: DMF and DMF + EtOH. (A) 27 g of polymer dissolved in DMF doped with 0.1 wt.% of TiO_2. (B) 27 g of polymer dissolved in DMF doped with 0.2 wt.% of TiO_2. (C) 27 g of polymer dissolved in DMF + EtOH 1% doped with 0.1 wt.% of TiO_2. (D) 27 g of polymer dissolved in DMF + EtOH 1% doped with 0.2 wt.% of TiO_2.

ative surface charge of TiO_2 particles increased. These results indicate that the TiO_2 particles have a lower tendency of agglomeration when they are electrically charged. The solution pH affects the hydrodynamic diameter of TiO_2 nanoparticles by changing the particle's surface charge and zeta potential [32].

The dispersion hydrodynamic diameter is controlled by nanoparticle agglomeration in the aqueous system. In the classical Derjaguin–Landau–Verwey–Overbeek (DLVO) theory, the agglomeration of nanoparticles is determined by the sum of the repulsive electrostatic force (the interaction of electrical double layer surrounding each nanoparticle) and the attractive van der Waals force [33,34].

Near the IEP, significant agglomeration takes place; large flocs are observed, as the particle surface charge is close to zero, and attractive van der Waals forces are dominant. When the pH is significantly different from IEP for titania, the absolute value of zeta potential becomes higher and the hydrodynamic size of agglomerates becomes smaller.

Agglomeration of TiO_2 nanoparticles can dominate when the solution pH (ca. 6.2) is close to the IEP because the repulsive force between nanoparticles caused by electrostatic interaction can be mitigated [35].

Subsequently, the effect of EtOH addition on the particle size distribution was explored but measured in the polymeric solutions used for membrane synthesis. The size of TiO_2 particles plays an important role on the hindrance effect of particles during the membrane synthesis process. This effect, as explained in the Introduction section, reduces the interaction between polymer and solvent molecules promoting membranes with higher pore size and porosity [25,26].

It is well-known that the nano-TiO_2 particles show a tendency to aggregate due to their high specific surface area and the hydroxyl groups on the TiO_2 surface [36]. The observed size distribution of the nanoparticles in polymeric solutions at different contents of TiO_2 is shown in Fig. 4.

EtOH is usually used as a particle dispersant in aqueous solutions because it causes an increasing of surface potential of particles, thereby decreasing the tendency to aggregation [37]. However, in this case, the pH of the modified polymeric solution after EtOH addition was 8, lower than the pH of former DMF polymeric solution (pH 9). The isoelectric point of TiO_2 is close to neutral pH. According to the results shown in Fig. 3, at a pH closer to the IEP, the decreased electrostatic repulsion between nanoparticles favored the formation of aggregates having larger size. This change in pH removes the repulsive forces determined by electrical double layer (EDL) that keep colloidal particles separate and allows for flocculation due to van der Waals forces.

However, in non-aqueous systems (polymeric solution), the electrostatic charge on the particle surface decreases with decreasing dielectric constant of medium between particles (Table 1). The addition of EtOH to the solvent media DMF alters the dielectric constant of media. For the mixture, the dielectric constant is around 40, slightly lower than dielectric constant of pure DMF (41.3). The dielectric constant measures the solvent ability to reduce the field strength of the electric field surrounding a charged particle immersed in it. So, the order from dispersion to flocculation should agree with the order of dielectric constant of the solvents. It is expected that as a result of the addition of ethanol to the dispersion medium, a decrease of the dielectric constant of the solvent mixture is obtained, so that the size of flocs increases.

Another possible explanation is that the effect on the surface potential as result of EtOH addition is mitigated by the presence of polymer chains. If there are polymer chains inside the system and particularly PES because of its rod-like structure and the totally negative charge distribution over the chain that it has, when it locates between two TiO_2 particles with OH— on the surface, it will be rejected from the particle gap. The zone between the particles is depleted from the polymer chains, and it increases the osmotic pressure in the surrounding of the particles, which pushes them to form aggregates, as it is shown in the Fig. 5.

So, in this case, the possible increase in the surface potential caused by EtOH addition will be suppressed by increase in the osmotic pressure, $\prod$, and the distance between two particles reached the value that in which the van der Waals is dominated over the EDL force and as a result we will get the aggregates. This effect is known as depletion in the suspension field [38]. It can be questioned that the same effect should be observable in the suspension system of DMF and nanoparticles, the reason why the depletion effect is not pronounced as it is in the case of EtOH is the presence of two competing effects as it is shown also in the Fig. 5. First, evacuation of zones between the particles, which is an entropic driven phenomenon and second, the electrostatic force between particle surface and the polymer chain which in the case of DMF and nanoparticle is attractive, due to the pH of system which is higher than the pH of IEP, and suppressing the depletion of the particles. In contrast, the presence of EtOH results in decreasing the pH and inducing the negative charge over the particle surface, which change the electrostatic force to repulsion and favors the depletion and as a result agglomoration of the particles.

Finally, addition of EtOH will not enhance the particle dispersion due to two main reasons:

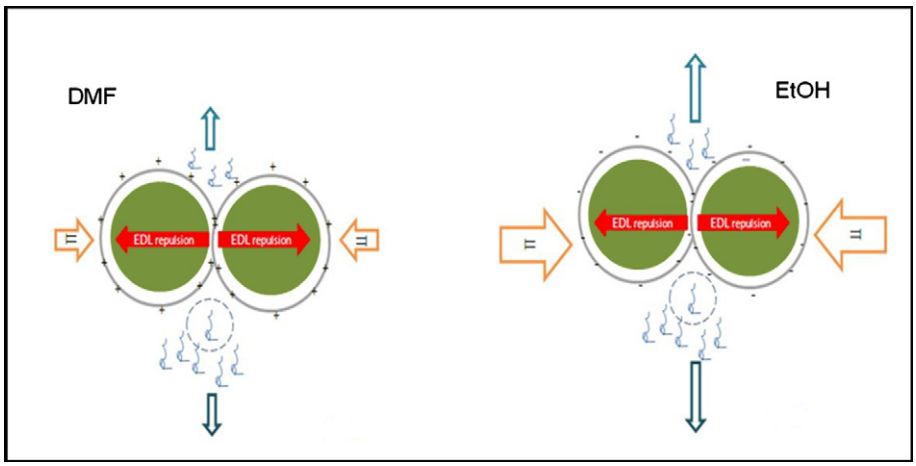

Fig. 5. Depletion of suspension field of particles.

(i) Decrease of the dielectric constant of solution.
(ii) Depletion of the suspension field determined by the interaction of polymer chains and surroundings.

3.2. Membrane morphology

Analysis by SEM provides a visual and quantitative characterization of the surface morphology of unmodified and modified adding TiO_2 membranes (Fig. 6).

The addition of TiO_2 to the polymeric solution results in the increase of the macrovoid dimensions as well as suppressing the sponge-like structure of the membrane [23]. The higher presence of macrovoids with a finger-like structure is postulated to be associated with the hindrance effect of nanoparticles during the phase inversion process. Due to the interfacial stress between polymer and nanoparticles, interfacial pores are formed as consequence of shrinkage of polymer phase during the demixing process [6,39,40].

Cross-section images given in Fig. 7 show the TiO_2 concentration effect and the influence of EtOH used as additional solvent (1 wt.%) on the membrane morphology. As a consequence of the increase of the nanoparticle concentration from 0.1 to 0.2 wt.%, two different effects can be observed: the macrovoids length increases to around 20 μm, a structure with less macrovoids is obtained. These findings can be explained in terms of nanoparticle agglomeration: as result of the concentration increase, the nanoparticle cluster size increases, decreasing the number of clusters that interact with the polymer phase during phase inversion. As a result of EtOH addition, comparing images 7a and 7c, the length of macrovoids also increases but the number of macrovoids is hardly affected. The use of ethanol favors the flocculation of nanoparticles and hence the formation of higher pore sizes on the membrane surface (Fig. 4).

Comparing the images shown in Fig. 6, it can be concluded that the effect of the TiO_2 concentration was higher than the solvent effect in the formation of TiO_2 clusters. However, the increase of macrovoid dimensions was rather similar.

3.3. Membrane hydrophilicity

A series of membranes was subjected to contact angle measurements. Standard deviations obtained on a single sample are of the order of a few degrees, which represent an acceptable reproducibility. In Fig. 8, the images of water droplets in contact with the surface of unmodified and modified membranes are shown.

A strong correlation exists between the orientation (geometry) of water at a solid–liquid interface and the hydrophilicity of the solid surface [41,42]. The restructuring of interfacial water molecules can explain the observed increase in hydrophilicity as depicted in Fig. 7. First, the increased ordering of the interfacial water molecules improves the water molecule's ability to form hydrogen bonds and, in turn, produces stronger interactions between water and the solid phase (membrane surface).

The contact angles values shown in Fig. 9A decrease with increasing TiO_2 concentration until 0.2 wt.%, varying almost linearly. At this concentration, the hydrophilicity through the membrane surface rather increases. So, there are two well-defined behaviors associated to different concentration ranges. The addition of EtOH to the polymeric solution resulted in a decrease of

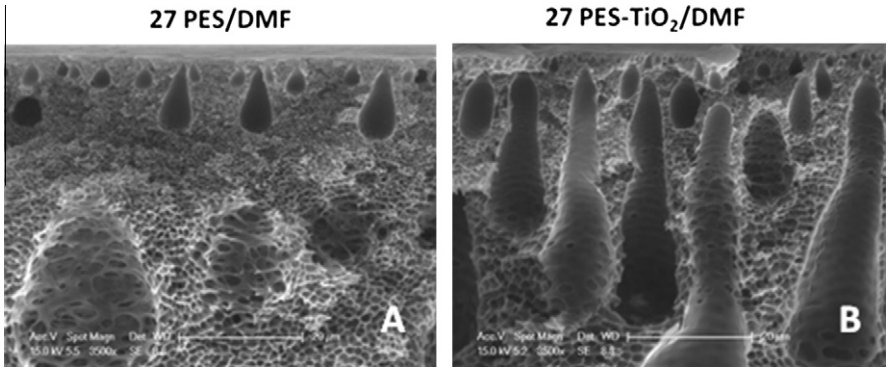

Fig. 6. SEM images of the control PES membrane and modified PES–TiO_2 membrane. (A) Control: 27 g of polymer dissolved in DMF. (B) Modified: 27 g of polymer dissolved in DMF doped with 0.1 wt.% of TiO_2.

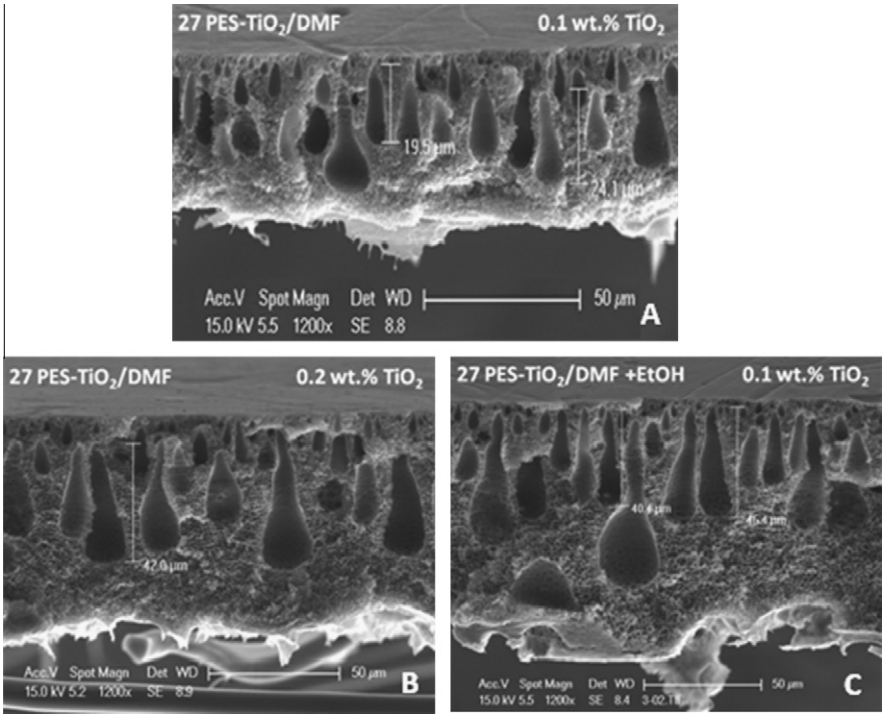

Fig. 7. SEM images of the PES–TiO_2 membranes at different concentration of TiO_2 and EtOH. (A) 27 g of polymer dissolved in DMF doped with 0.1 wt.% of TiO_2. (B) 27 g of polymer dissolved in DMF doped with 0.2 wt.% of TiO_2. (C) 27 g of polymer dissolved in DMF + EtOH 1% doped with 0.1 wt.% of TiO_2.

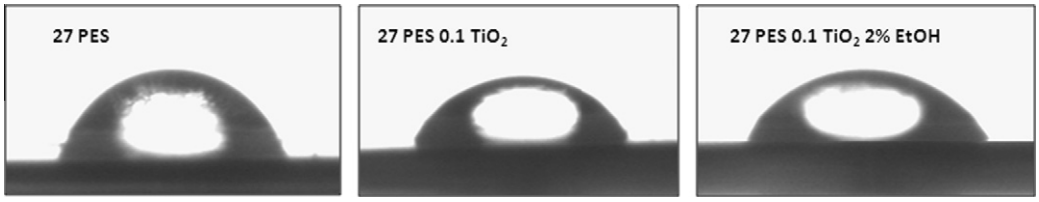

Fig. 8. Images of water droplets taken for different membranes surface (solid phase).

contact angle values showing a similar behavior for two different contents of TiO_2 (Fig. 9B). This fact indicates that the addition of EtOH has a large and positive effect on the membrane hydrophilicity at concentrations below 2%, the decreasing trend of the contact angle values disappeared at higher contents of EtOH. It is important to point out that the membrane hydrophilicity improvement shows limit values as function of TiO_2 and EtOH concentrations.

Considering constant polymer and TiO_2 concentrations, the observed decrease of the contact angles as a function of the EtOH concentration is related to an increase of pore size during the solvent–non-solvent demixing process. It is expected that as result of the increase of the pore diameter, more water should be adsorbed by the membrane structure during the contact angle experiments. The addition of EtOH to the polymeric solution should promote the nanoparticle agglomeration and hence the formation of larger size TiO_2 clusters. Thus, it can be concluded that the formation mechanism of TiO_2-blended membranes is altered, in a similar way, at two low contents of nanoparticles (0.1% and 0.2%) by the addition of EtOH as co-solvent for the membrane preparation. However, at concentrations of EtOH above 2%, the contact angle of the membranes rather increases.

3.4. Membrane characterization

The physicochemical properties and performance of PES/TiO_2 membranes vary considerably with the conditioning treatment. In this study, the hydraulic permeability and porosity were measured as a function of membrane conditioning. The results shown in Fig. 10 are the average of 16 experimental values, and the trends were above the experimental error (5% and 8% for control and modified membranes, respectively).Two different experimental sets were carried out: (1) to study the influence of TiO_2 concentration, different contents of nanoparticles were dissolved into the polymeric solution (Fig. 10A), and (2) to explore the effect of EtOH, different volumes of EtOH were added for two different concentrations of TiO_2: 0.1 and 0.2 wt.% (Fig. 10B).

As a result of the addition of increasing concentrations of TiO_2, the permeability increased for lower contents of nanoparticles (Fig. 9A).

At concentrations above 0.2 wt.%, the permeability decreased. This trend is in agreement with contact angle measurements shown in Fig. 8A. Fig. 10B also shows an apparent maximum in the water permeation rate of membranes for two different TiO_2 contents by addition of EtOH as co-solvent. The shape of curves is similar for both experimental sets. First, it is observed again that the use of EtOH as co-solvent alters the membranes performance in the same way. Secondly, it is possible to accomplish improvements in the membrane permeability without further additions of nanoparticles: the permeation value obtained for the membrane doped at 2% of TiO_2 was similar to the corresponding value to the membrane doped at 1% of TiO_2 manufactured with EtOH as polymer co-solvent (rectangular marked in Fig. 10B). Thirdly, for EtOH con-

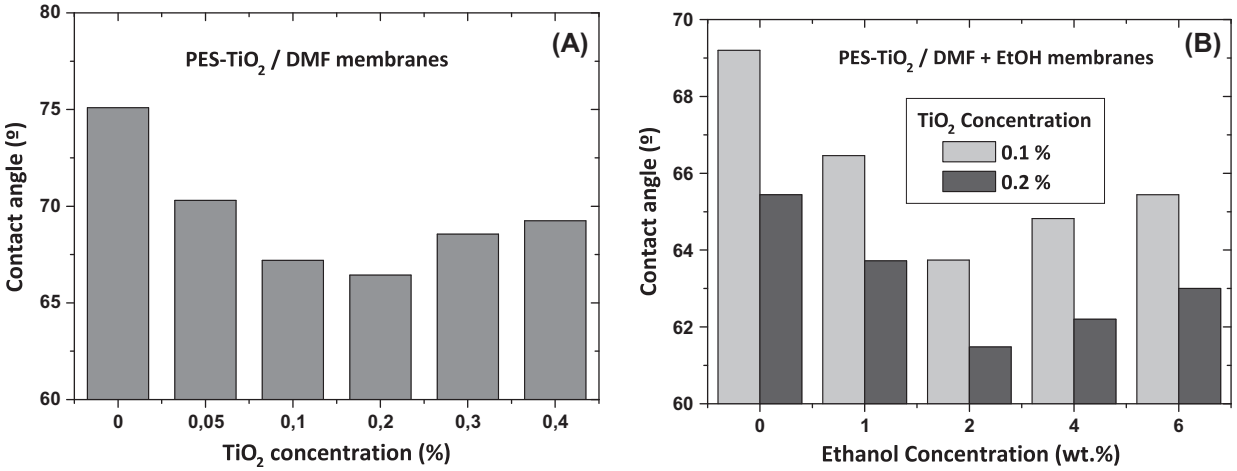

Fig. 9. Contact angles measurements of modified membranes as function of TiO_2 (A) and EtOH (B) concentrations.

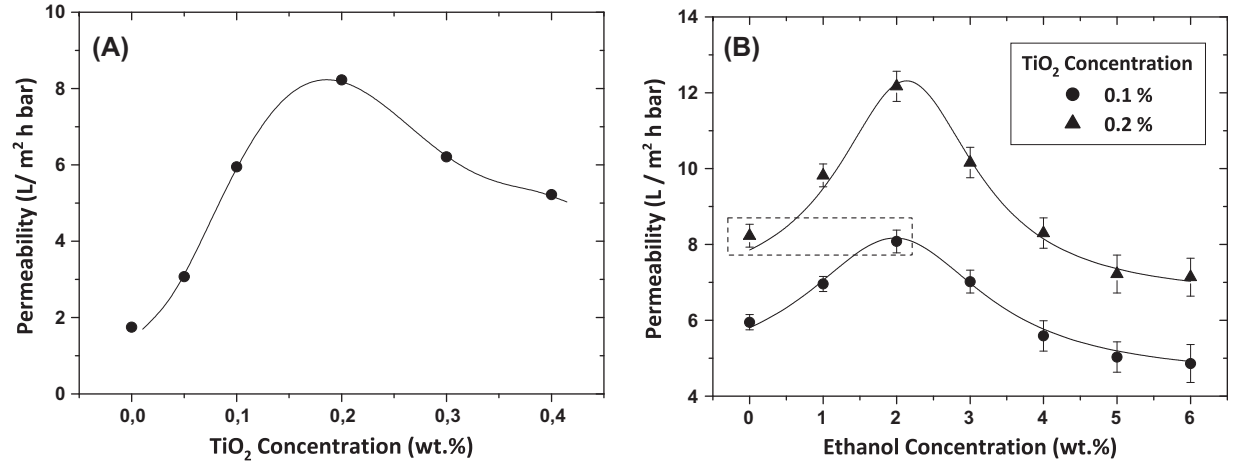

Fig. 10. Effects of TiO_2 and EtOH on pure water permeation. (A) PES–TiO_2/DMF membranes as function of TiO_2 concentration. (B) PES–TiO_2/DMF + EtOH membranes as function of EtOH concentration.

centrations above 4%, the improvement in the membrane permeability disappears. The results shown in Fig. 10 demonstrate the importance of agglomeration and a rigorous evaluation of agglomerates rather than simple determination of primary particle sizes from TEM observations. On the other hand, it is also important to point out that the overall behavior shown during both experimental sets (TiO_2 and EtOH concentration analyses) was similar.

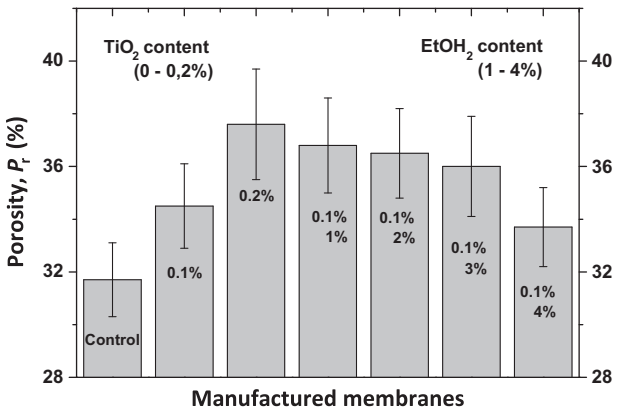

Fig. 11. Membrane porosity as function of TiO_2 and EtOH concentrations.

In Fig. 11, the uptake water experiments are shown, expressed as a function of membrane porosity. Higher amounts of absorbed water by the increasing TiO_2 doped membranes are explained in terms of hydrophilicity and increase of structural vacancies into the polymeric material. In order to discriminate between the effects of the two variables involved in these experiments (TiO_2 and EtOH concentrations), a further analysis will focus on the influence of the EtOH content. Comparing two membranes (with identical percentage of nanoparticles) without and with EtOH addition, at concentrations below 3%, an increase of membrane porosity can be observed. This could be related with the observed increase of macrovoid dimensions into the morphology of membranes (Fig. 7). As the vacancies volume into the membrane structure increases, the absorbed water amount should be higher. It is interesting to note that an optimum value is observed for the EtOH content (1–2%) in good accordance with the maximum observed for the permeability experiments. At concentrations above 3% of EtOH, both the permeability (Fig. 10) and porosity (Fig. 11) decrease, showing experimental values similar to those observed for the control membrane, manufactured without any modification. Some authors associate a decrease of membrane improvement to pore blocking or formation of stressed points as result of formation of high nanoparticles aggregates [6,11,39]. However, a similar performance observed in control and "highly-modified" membranes suggest that as a consequence of nanoparticles aggregation, the larger

Table 2
TiO_2 concentration in membrane structure by ICP-AES.

TiO_2 content in casting solution (wt.%)	EtOH content in casting solution (wt.%)	Expected TiO_2 in membrane (wt.%)	Calculated TiO_2 in membrane (wt.%)
0.1	0	0.37	0.55
0.2		0.74	0.89
0.4		1.46	1.36
	1		0.50
0.1	2	0.37	0.48
	4		0.31

size TiO_2 cluster formed cannot be entrapped by the polymer network or these aggregates precipitate during the phase inversion process due to the high cluster weight. So, the nanoparticle incorporation into the polymer matrix appears to be really poor for the membranes manufactured with high nanoparticles aggregates, whatever is the source of cluster formation, TiO_2 concentration or additional co-solvent.

Previous work [21] has demonstrated that an increase of dispersed nanoparticles into the polymeric solution, in the low concentration interval, promotes an increase of membrane porosity.

The presence of TiO_2 nanoparticles into the polymer matrix was confirmed by ICP-AES measurements. Table 2 shows the relation between expected and observed concentrations of TiO_2 into the manufactured membrane composition.

At lower contents of TiO_2, the calculated concentrations from ICP measurements were higher than expected values. This fact could be caused by non well dispersion of nanoparticles in every manufactured membrane sheet. However, at 0.4 wt.% of TiO_2, the final content in the polymer matrix is lower than expected. This fact is also common for the highest percentage of EtOH (4 wt.%). Considering that the increase of both nanoparticles and EtOH contents into the polymeric solution causes a similar effect: increase of nanoparticle size, the observed results at higher contents of both variables could be related with a poor entrapment potential of polymer matrix as consequence of high clusters size. A fraction could enter the aqueous phase during phase separation.

3.5. Thermal resistance of hybrid membranes

The thermal performance of manufactured membranes, as determined with TGA, is shown in Fig. 12. The thermal stability of control and TiO_2-entrapped membranes at different particle content can be seen in this figure.

As shown in Fig. 12, the manufactured membranes have a good thermal resistance. The decomposition temperature (T_d, defined as the temperature at 3% weight loss) for the selected membranes was around 430 °C. This result is coherent with reported values in the literature [13]. For TGA curves shown in Fig. 12, the T_d weakly increased (around 10 °C) as consequence of nanoparticles incorporation into the polymer matrix. The rate of decomposition of the modified membrane increased slightly, this fact can be interpreted as the polymer chains movements during heating is restricted with the introduction of TiO_2 particles. A small increase is observed for the residual weight of PES–TiO_2/DMF membranes at temperatures above 600 °C.

Considering that the residual weight obtained for the control 27 PES membrane at 650 °C is around 11%, leaving a thermostable residue, the difference between the percentages of the original membrane and the membranes to which TiO_2 was added should be related to the TiO_2 fraction added. The ratios of residual for PES–TiO_2 membranes were around 13% and 16% for the 0.1 and 0.2 wt.% of TiO_2, respectively.

In order to estimate rigorously the real effect of TiO_2 incorporation on the thermal stability of membranes, it was determined by TGA the weight loss of just the TiO_2 powder. The obtained percentage was around 0.7%.

Calculating the differences between residues of control and modified membranes and subtracting to them, the percentage corresponded to TiO_2 yields an estimate of 1% and 3% of residues for samples of membranes doped at 0.1 and 0.2 wt.% of TiO_2, respectively. These values are not in the concentration expected ranges (Table 2). This fact suggests inhomogeneity of TiO_2 dispersion or that the polymeric cross-linking density increases as result of addition of inorganic particles and the corresponding variation of thermal resistance could not be in a direct proportion with increase of inorganic particles into the PES matrix.

3.6. Fouling mitigation effect of TiO_2 and EtOH

In order to explore the influence of addition of TiO_2 nanoparticles in the low concentration interval and the effect of ethanol as co-solvent into the casting solution composition, the experiments shown in Fig. 13 were performed.

The incorporation of nanoparticles into the polymer matrix causes an increase of membrane fouling resistance. Fig. 12 proves the antifouling effect: fouling of the TiO_2 entrapped membrane was significantly reduced compared to that of the control PES/DMF membrane. The flux declined fast and gradually at the begin-

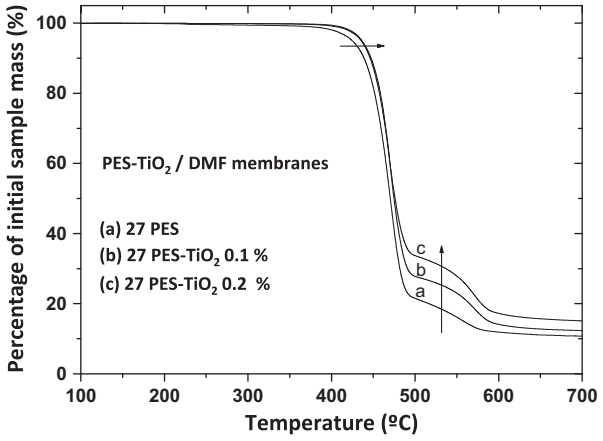

Fig. 12. TGA curves of the control 27 PES membrane and PES–TiO_2 modified membranes.

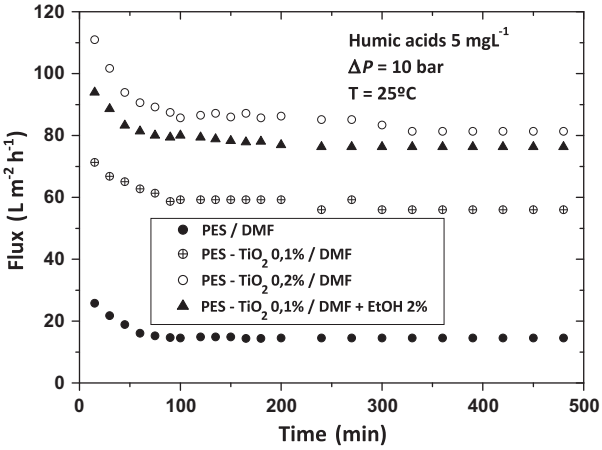

Fig. 13. Membrane fouling experiments: addition effect of TiO_2 and EtOH.

Table 3
Filtration resistances for control and modified membranes.

Membrane	R_m ($\times 10^7$) m^{-1}	R_f ($\times 10^7$) m^{-1}	R_g ($\times 10^7$) m^{-1}	R_t ($\times 10^7$) m^{-1}
PES/DMF	227	25.5	25.5	278
PES–TiO_2 0.1%/DMF	67	2.9	2.5	72
PES–TiO_2 0.2%/DMF	48	0.6	0.8	50
PES–TiO_2 0.1%/ DMF + EtOH 2%	49	1.3	2.5	53

ning of filtration for all membranes, after 100 min of filtration time all membranes showed a steady state in the permeation rate.

Mitigation of fouling phenomena during separation of organic foulants can be assessed by changing the hydrodynamic conditions or enhancing the hydrophilicity of membrane surface [18,43]. Taking into account that the experiments shown in Fig. 13 were all carried out at the same operational conditions, the observed increase in the mitigation of membrane fouling should be associated to membrane surface modification. In this sense, as a result of increasing nanoparticle content into the polymeric solution, the concentration of TiO_2 clusters throughout the membrane surface increases and hence leads to an improvement of hydrophilicity that gives rise to the inhibition of hydrophobic interactions between the membrane surface and organic foulants [44,45]. The results shown in Table 3 clearly show that the filtration resistances significantly decreased as a result of the TiO_2 load.

The effect of the TiO_2 adding can be readily discerned from the observed differences between intrinsic membrane resistances (R_m) obtained for control and modified membranes. Furthermore, the relative fouling resistance determined by solute adsorption of foulants on membrane pore wall or surface (R_f) is more than 9% of the total resistance of the control membrane, whereas for the PES–TiO_2/DMF membranes doped at 0.1and 0.2 wt.% of TiO_2 are 4% and 1% of their R_t. Similar percentages are observed for the relative membrane resistance R_g. Hence, the incorporation of TiO_2 mitigates considerably the hydrophobic interactions in the interface organic foulants–membrane surface that could lead to the foulants adsorption or hydrophobic layer formation. For the membrane doped at 0.1 wt.% of TiO_2 synthesized with ethanol as co-solvent, the percentages of R_f and R_g respect to total membrane resistance are around 3% and 4%, respectively. Therefore, the fouling resistance of PES membranes is not only improved by incorporation of nanoparticles, but also by using EtOH as co-solvent. Comparing both effects, it is evident that the addition of nanoparticles has a larger impact than the EtOH effect, especially for gel formation resistance (R_g) that does not change by the EtOH effect. However, the foulant adsorption (R_f) is less pronounced for membranes synthesized with ethanol as co-solvent.

3.7. Rejection performance

The influence of the addition of TiO_2 and EtOH to the polymer casting solution on the rejection of solutes was assessed by filtration experiments of PEGs with different molar mass as shown in Fig. 14. In order to compare the rejection potential of tested membranes, the molecular weight cut-off (MWCO) of membranes was determined.

In Fig. 14, the obtained values of MWCO for the tested membranes are shown. The observed small increase of MWCO for modified membranes in comparison with the control 27 PES/DMF membrane can be explained in terms of pose size increasing. Considering the steric exclusion as the most important mechanism during PEGs filtration experiments, the rate of solute rejection should be determined by the ratio of pore and solute dimensions [24]. These observations are consistent with the permeability increase obtained for modified membranes (Fig. 9).

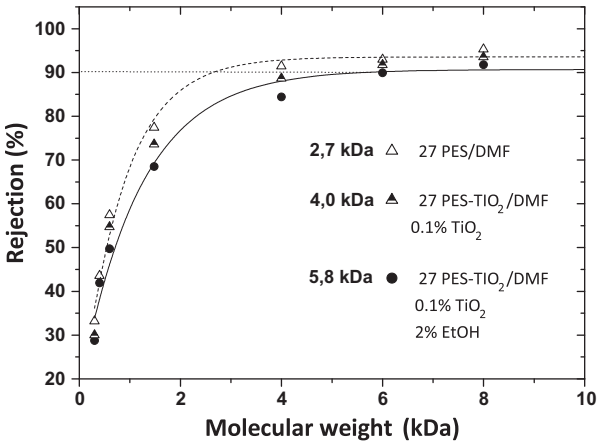

Fig. 14. Molecular weights cut-off for control and modified membranes.

4. Conclusions

This study aimed at improving the overall membrane performance, especially its fouling resistance by incorporation inside the polymer matrix of small amount of nanoparticles and also to show the use of EtOH as polymer co-solvent. The main findings from this research are:

1. Zeta potential measurements in aqueous solution demonstrated as the TiO_2 particles size is dominated by EDL interactions.
2. Particle size distributions determined for polymeric solutions showed that addition of EtOH did not improve the rate of particle dispersion but the clusters size was increased as consequence of a double effect: reduction of the dielectric constant of solution and the depletion of the suspension field determined by the action of the polymer chains.
3. The modified membranes by TiO_2 incorporation showed a structural change from a sponge-like to a finger-like structure. The observed effects as result of EtOH addition and increase of TiO_2 concentration were similar: both procedures provoked an increase of macrovoid dimensions. The resulted membrane structure was more porous. This fact was confirmed by uptake water experiments.
4. Strong correlations were observed between the hydrophilicity and the permeability of manufactured membranes. The formation mechanism of TiO_2-blended membranes was altered, in a similar way, as result of EtOH at different contents of nanoparticles. The improvement of membrane permeation can be assessed in a similar extent either by incorporation of higher content of TiO_2 or adding a specific amount of EtOH as result of particle aggregation.
5. In agreement with physico-chemical characterization of membranes, the fouling resistance of modified membranes was significantly improved showing that EtOH addition is a suitable procedure for the membrane performance improvement.
6. The rejection potential of membranes is hardly affected by the nanoparticles and EtOH incorporation into the polymeric solution.

Acknowledgments

This research was supported by Basic Science Research Program through the National Research Foundation of Korea (NRF) funded by the Ministry of Education, Science and Technology (2010-0024286).

Arcadio Sotto would like to acknowledge the support provided by the Regional Government of Madrid through Project REMTAV-ARES (S2009/AMB-1588) and Mr. Juan Manuel Suárez Muñoz for performing the ICP measurements.

References

[1] J. Kim, B. Van der Bruggen, Environ. Pollut. 158 (2010) 2335.
[2] Y. Mansourpanah, S.S. Madaeni, A. Rahimpour, A. Farhadian, A.H. Taheri, J. Membr. Sci. 330 (2009) 297.
[3] N. Maximous, G. Nakhla, W. Wan, K. Wong, J. Membr. Sci. 341 (2009) 67.
[4] S.L. Yu, X.T. Zuo, R.L. Bao, X. Xu, J. Wang, J. Xu, Polymer 50 (2009) 553.
[5] N. Maximous, G. Nakhla, W. Wan, K. Wong, J. Membr. Sci. (2010) 222.
[6] A. Rahimpour, S.S. Madaeni, A.H. Taheri, Y. Mansourpanah, J. Membr. Sci. 313 (2008) 158.
[7] S.J. Oh, N. Kim, Y.T. Lee, J. Membr. Sci. 345 (2009) 13.
[8] J. Shen, H. Ruan, L. Wu, C. Gao, Chem. Eng. J. 168 (2011) 1272.
[9] A. Rahimpour, S.S. Madaeni, J. Membr. Sci. 360 (2010) 371.
[10] N.A.A. Hamid, A.F. Ismail, T. Matsuura, A.W. Zularisam, W.J. Lau, E. Yuliwati, M.S. Abdullah, Desalination 273 (2011) 85.
[11] G. Wu, S. Gan, L. Cui, Y. Xu, Appl. Surf. Sci. 254 (2008) 7080.
[12] M. Luo, W. Tang, J. Zhao, C. Pu, J. Mater. Process. Technol. 172 (2006) 431.
[13] J.-F. Li, Z.-L. Xu, H. Yang, L.-Y. Yu, M. Liu, Appl. Surf. Sci. 255 (2009) 4725.
[14] R. Molinari, M. Mungari, E. Drioli, A.D. Paola, V. Loddo, L. Palmisano, M. Schiavello, Catal. Today 55 (2000) 71–78.
[15] R. Molinari, C. Grande, E. Drioli, L. Palmisano, M. Schiavello, Catal. Today 67 (2001) 273–279.
[16] A. Bottino, G. Capannelli, V. D'Asti, J. Sep. Purif. Technol. 22–23 (2001) 269–275.
[17] J.C. Yu, J. Yu, W. Hoa, J. Zhao, J. Photochem. Photobiol. A 148 (2002) 331.
[18] T.-H. Bae, I.-C. Kim, T.-M. Tak, J. Membr. Sci. 275 (2006) 1.
[19] E. Yuliwati, A.F. Ismail, Desalination 273 (2011) 226.
[20] R.A. Damodar, S.-J. You, H.-H. Chou, J. Hazard. Mater. 172 (2009) 1321.
[21] A. Sotto, A. Boromand, S. Balta, J. Kim, B. Van der Bruggen, J. Mater. Chem. 21 (2011) 10311.
[22] K. Suttiponparnit, J. Jiang, M. Sahu, S. Suvachittanont, T. Charinpanitkul, P. Biswas, Nanoscale Res. Lett. 6 (2011) 1.
[23] A. Razmjou, J. Mansouri, V. Chen, J. Membr. Sci. 378 (2011) 73.
[24] N. Maximous, G. Nakhla, W. Wan, K. Wong, J. Membr. Sci. 361 (2010) 213.
[25] M. Mulder, Basic Principles of Membrane Technology, Kluwer Academic Publishers, 1996. p. 383.
[26] I.C. Kim, K.H. Lee, T.M. Tak, J. Membr. Sci. 183 (2001) 235–247.
[27] K. Listiarini, D.D. Sun, J.O. Leckie, J. Membr. Sci. 332 (2009) 56.
[28] M.A. Zazouli, S. Nasseri, M. Ulbricht, Desalination 250 (2010) 688.
[29] B. Van der Bruggen, K. Everaert, D. Wilms, C. Vandecasteele, J. Membr. Sci. 193 (2001) 239.
[30] S. Quorzal, A. Assabbane, Y. Ait-Ichou, J. Photochem. Photobiol. A: Chem. 163 (2004) 317.
[31] S.H. Kim, S.-Y. Kwak, B.-H. Sohn, T.H. Park, J. Membr. Sci. 211 (2003) 157.
[32] K. Suttiponparnit, J. Jiang, M. Sahu, S. Suvachittanont, T. Charinpanitku, P. Biswas, Nanoscale Res. Lett. 6 (2011) 27.
[33] B.V. Derjaguin, L.D. Landau, Acta Physicochim. URSS 14 (1941) 733.
[34] E.J.W. Verwey, J.T.G. Overbeek, Theory of the Stability of Lyophobic Colloids, Elsevier, Amsterdam, 1948.
[35] Z. Zhang, C.-C. Wang, R. Zakaria, J.Y. Ying, J. Phys. Chem. B 102 (1998) 10871.
[36] H. Lin, C.P. Huang, W. Li, C. Ni, S. Ismat Shah, Yao-Hsuan Tseng, Appl. Catal. B 68 (2006) 1.
[37] M. Fuchs, K.S. Schweizer, J. Phys.: Condens. Matter 14 (2002) R239.
[38] K.D. Kim, H.T. Kim, J. Eur. Ceram. Soc. 23 (2003) 833.
[39] Y. Yang, H. Zhang, P. Wang, Q. Zheng, J. Li, J. Membr. Sci. 288 (2007) 231.
[40] H. Susanto, M. Ulbricht, in: E. Drioli, L. Giorno (Eds.), Membrane Operations. Innovative Separations and Transformations, Wiley-VCH, Weinheim, 2009, pp. 26–30.
[41] G. Hurwitz, G.R. Guillen, E.M.V. Hoek, J. Membr. Sci. 349 (2010) 349.
[42] Q. Du, E. Freysz, Y.R. Shen, Science 264 (1994) 826.
[43] B. Van der Bruggen, M. Mänttäri, M. Nyström, Sep. Purif. Technol. 63 (2008) 251.
[44] L. Braeken, K. Boussu, B. Van der Bruggen, C. Vandecasteele, ChemPhysChem 6 (2005) 1606.
[45] J.M. Arsuaga, A. Sotto, M.J. López-Muñoz, L. Braeken, J. Membr. Sci. 372 (2011) 380.